Noise estimation and probability of detection in non-resolved images: application to space object observation

Francois Sanson, Carolin Frueh

Noise estimation and probability of detection in non-resolved images: application to space object observation

Francois Sanson[a,*], Carolin Frueh[b]

[a] *DEFi Team (Inria Saclay IDF, Ecole Polytechnique), CMAP Lab, Route de Saclay, 91120 Palaiseau, France*
[b] *Assistant Professor at School of Aeronautics and Astronautics, Purdue University, West Lafayette IN 47906, USA*

Abstract

Charged Couple Device (CCD) technology is widely used in various scientific measurement contexts. CCD equipped cameras have revolutionized astronomy and space-related optical telescope measurements in recent years. They are also used in electroscopic measurements, e.g., in fields such as geology, biology, and medicine. The signal-to-noise ratio and the probability of detection are crucial to design experiments observation setups properly and to employ further mathematical methods for data exploitation such as, e.g. multi-target tracking methods. Previous attempts to correctly characterize the signal-to-noise ratio for star observations are revisited in this work and adapted for the application of near-Earth object observations and high precision measurements, leading to a modified CCD equation. Our formulation proposes a novel distribution of the signal noise that accurately accounts for the truncation noise and the presence of ambiguous pixels. These improvements are employed to derive the probability of detection and the SNR with significant improvements compared to existing formulations when ambiguous pixels are present.

Keywords: Space Situational Awareness ; Signal Processing ; Optical Astronomy ; CCD

*Corresponding author. Tel.: +33(0)5 24 57 41 12
Email address: francois.sanson@inria.fr (Francois Sanson)

1. Introduction

Since its introduction in the early seventies, Charged Coupled Device (CCD) technology revolutionized optical measurements in both consumer market and scientific imaging alike. In non-resolved imaging, details of the objects or structures of interest are not available. Such images are encountered in Astronomy or Medical imaging Smal et al. (2010). The object image is represented by one to a couple of hundred pixels that stand out from the background. In practice, working with non-resolved images raise several challenges: first, the object pixels have to be discriminated from the noisy background of the whole frame. The background is typically composed of clutter or spurious object images, sometimes with the same intensity as the signal of interest. In this case, the object signal does not clearly stand out from the background and may remain undetected. Second, the sensing process itself is a stochastic process affected by noise that deteriorates our ability to single out object signal.

A CCD sensor is usually composed of a thin layer of photoactive semi-conductors (typically silicons) and a transmitter region (see Janesick et al. (1987) for a complete review of CCD functioning). The photon bombardment leads to electron emissions according to a stochastic process that yields different results from one observation to another. The electrons are collected in a capacitor well at each so-called pixel. After the photo exposure, a control circuit performs the readout of the CCD, during which each capacitor transfers its charge to the neighboring pixel. The electrons are transferred to a voltage level. This readout process is subject to random errors that directly affect the resulting image. Hence the obtained signal image is the realization of a series of complex random processes which affect our ability to detect and track space objects Massey and George (1992). Furthermore, hot and dead pixels can lead to false detections if they are not masked. Hot pixels constantly show a signal (charge) even when the camera shutter is closed while dead pixels do not measure any signal.

The community worked on deriving estimates of the Signal-to-Noise Ratio

(SNR) and the probability of detection to quantify and predict the expected information obtained from an observation beforehand. The SNR is the expected intensity of a signal divided by the expected noise associated with the signal. The probability of detection is the probability that an object is detected for a given scenario. Several approaches have been developed to estimate both quantities. One method consists in simulating a large number of CCD output realizations of the same observation to extract an average SNR and probability of detection for each observation scenario. Such Monte Carlo approaches are in particular proposed in Merline and Howell (1995) where a computer simulator of a CCD is presented. The accuracy of the strategy depends on the number of samples that can be generated for each scenario. The major drawback of Monte Carlo methods is their computational cost: when a large number of observation scenarii has to be processed, they may become irrelevant because too computationally expensive. Alternatively, analytical approximations of the SRN have been proposed in the literature. The so-called 'CCD equation' is presented in its most classical form in the reference Howell (2006); Mortara and Fowler (1981). The CCD equation has been subsequently improved in Merline and Howell (1995) where the background subtraction noise is included. In Newberry (1991), the author proposes a CCD equation in the context of data reduction techniques (processing noise) and derives a model for the truncation noise.

Initially developed in the context of astronomical star observations, the expressions have certain shortcomings, especially when dealing with faint object images Merline and Howell (1995). Faint detections are frequent in the observation of near-Earth space objects and space debris objects in the field of Space Situational Awareness. Objects do not necessarily have a stable attitude, leading to time-varying detections. Nevertheless, precise and reliable estimations of the SNR and the probability are crucial inputs for object detection and tracking tasks. The SNR is an indication of the amount of information available in a signal. It is directly related for instance to the variance in the estimated space object position Sanson and Frueh (2019). Space Situational Awareness (SSA) heavily relies on ground observations to detect and track space objects. Automated

procedures need to be developed to identify and keep tracking hundreds of thousand objects. In recent years, space object tracking techniques have been greatly improved by the use of multi-object filtering approaches. Filtering algorithms (Kalman, Extended Kalman, Unscented,Probability Hypothesis Density) are classical tools for multi-object observation and tracking (see Mahler (2007) for reference) that have been adapted to SSA objectives Clark et al. (2007); McCabe et al. (2015); Delande et al. (2015); Clark et al. (2008); DeMars et al. (2015). All the mentioned algorithms strongly rely on the accurate and low-cost description of the SNR and the probability of detection. One other important aspect of SSA is the optimization of space object observation conditions to maximize the efficiency of a telescope or a network of telescopes. The algorithms proposed in Coder and Holzinger (2016); Frueh et al. (2017) directly use the SRN and probability of detection. Such optimization problems are typically non-convex and require the use of expensive genetic algorithms to obtain satisfying solutions.

In this work, we propose a novel derivation of the probability of detection and the SNR that can directly be used in tracking algorithms or design of optical observations. In the first step, previous methods of noise estimation, here called classical CCD equation are revisited (Section 2.1). Then a new analytical approximation of the signal-to-noise ratio is developed featuring more accurate modeling of the CCD truncation noise and ambiguous pixels for faint signals. The results are compared to the Monte Carlo simulations and existing CCD equations in Section 4.1. Besides, expressions for the probability of detection for the use in multi-target tracking frameworks are derived. The accurate statistical determination of noise and the probability of detection with fully analytic expression is crucial for a fast determination of a closed-form approximation of those quantities solely based on the physical situation without actually simulating a full frame image. The results eliminate the need to perform expensive Monte-Carlo simulations Preliminary studies on the topic have been performed by the authors in Sanson and Frueh (2015).

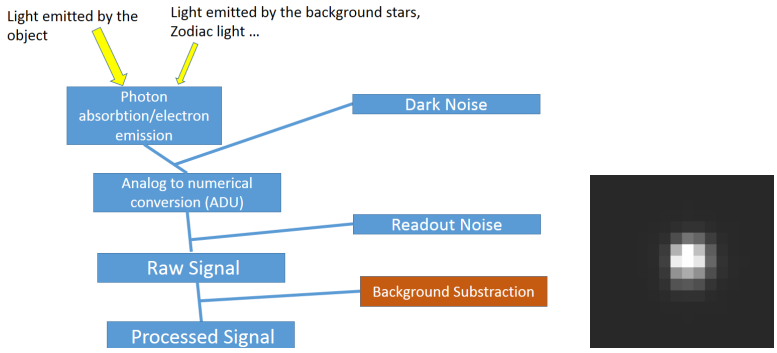

(a) signal generation (b) object image

Figure 1: a: Simplified signal generation processes on a CCD in ground-based astronomy observations. b: Space object image for an object with a relative movement to the observer and the signal obtained with a CCD, (source Purdue Optical Ground Station).

2. Estimation of the Signal-to-Noise Ratio (SNR)

The image generation process can be described as follow (see Fig.1a). All celestial light sources impinge on the sensor (object signal but also background stars, Zodiac light, etc.). The sensor itself generates spurious electrons called dark noise. For the signal to be read out, the readout process collects the electrons from each pixel and the analog to numeric conversion takes place. Additional noise is generated and referred to as readout noise. An example of a CCD generated image is represented in Fig.1b. The frame is cropped around the object image. Note that this is a high signal-to-noise ratio case. As the CCD image generation relies on photon absorption and electron emission, the resulting image is a stochastic process. Furthermore, to detect the object and find its centroid Hagen and Dereniak (2008); Sanson and Frueh (2019), the background has to be estimated and needs to be either locally or globally subtracted to the image Houtz and Frueh (2018). Background estimation itself introduces statistical error Merline and Howell (1995). To illustrate the stochastic nature of the signal generated by the CCD after background subtraction, Fig.2 shows three realizations of the same original light source, leading to three different realizations subject to the same stochastic processes.

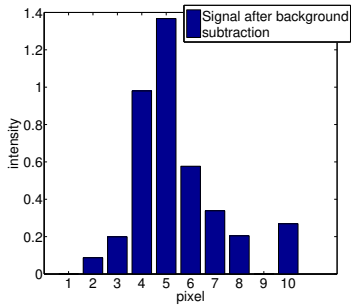

(a) Signal 1

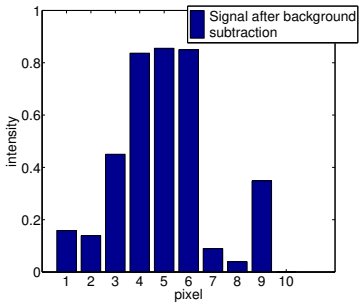

(b) Signal 2

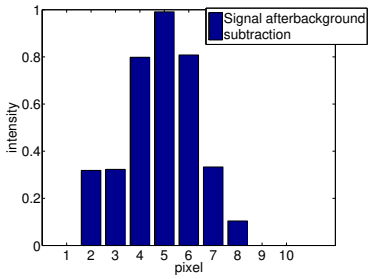

(c) Signal 3

Figure 2: Three observation realizations of the same object (light source signal), background noise, sensor-detector, and observation geometry, generated numerically and projected on x-direction for clarity.

Additional, higher order effects such as gain variations due to the CCD fabrication process or the brighter-wider effects have been noticed by several studies Lage et al. (2017); Beamer et al. (2015), but are neglected this paper.

Traditionally, the Signal-to-Noise Ratio (SNR) is referred to as the CCD equation. Signal-to-noise ratio is defined as the expectation value $\mathrm{E}(S)$ of a signal S over the standard deviation $\sqrt{\mathrm{var}(N)}$ of the noise N:

$$\mathrm{SNR} := \frac{\mathrm{E}(S)}{\sqrt{\mathrm{var}(N)}}, \tag{1}$$

Three different versions of the CCD equation are compared here: the classical $\mathrm{SNR}_{\mathrm{classic}}$ as in Tiersch (1993) , Merline's derived in Newberry (1991); Mer-

line and Howell (1995), $\mathrm{SNR}_{\mathrm{Merlin}}$, and our improved derivation formulation, $\mathrm{SNR}_{\mathrm{impro}}$, that is derived in this study. The assumptions of all three methods are discussed and compared.

2.1. Known Formulations of the CCD Equation

The signal of interest is the object signal S_{obj}, that is the trace that the object on the detector. The signal is usually computed by adding the signal intensity in all pixels i containing the object image. Theoretically, the object image is spread over the entire frame. Realistically, only the pixels above the background n are used. The SNR is then defined as the ratio between the sum of the signal intensities and the sum of the noise in each pixel:

$$S_{\mathrm{obj}} = \sum_{i}^{n_{pix}} S_{\mathrm{obj},i} \qquad N = \sum_{i}^{n_{pix}} N_i. \tag{2}$$

The noise N_i in a given pixel comes from distinct sources. It comes from the object signal $S_{\mathrm{obj},i}$, but also from the celestial and sky background sources $S_{\mathrm{S},i}$, such as stars, and other light sources: the zodiac light airglow and others, that contribute to a non-zero photo background. Furthermore, the dark noise, $N_{\mathrm{D},i}$, of the detector that results from atomic excitement in non-zero temperatures, and the readout noise $N_{\mathrm{R},i}$, of the detector contribute to the noise of the CCD output. The temperature of the detector influences both sources. Moreover, due to CCD limited resolutions, not every single electron can be reported. Inevitably there is a truncation noise introduced $N_{\mathrm{U},i}$. Then the total noise per pixel is:

$$N_{\mathrm{classic},i} = S_{obj,i} + S_{S,i} + N_{\mathrm{D},i} + N_{\mathrm{R},i} + N_{\mathrm{U},i} \tag{3}$$

The classical derivation concludes at these noise terms. The formulation of Merline and Howell (1995) adds a further term, stemming from the background estimation; it will be discussed below.

To determine mean and standard deviation for the SNR, the distributions of all those sources need to be determined. Here, there is a modeling choice given.

The basis of all three derivations is that the electron emittance after absorption of all incoming photons is modeled as a Poisson random variable (hypothesis 1). Incoming photons per pixel are stemming from the object itself per pixel i, $S_{\mathrm{obj},i}$ with mean and variance $\lambda_{\mathrm{obj},i}$ and from celestial and terrestrial background sources, $S_{\mathrm{S},i}$ with mean and variance $\lambda_{\mathrm{S},i}$. Furthermore the dark noise is also modelled as a Poisson variable $N_{\mathrm{D},i}$ with mean and variance $\lambda_{\mathrm{D},i}$. Thus:

$$\mathrm{E}[S_{\mathrm{obj}}] = \mathrm{var}(S_{\mathrm{obj}}) = \sum_{i}^{n_{pix}} \lambda_{\mathrm{obj},i}, \quad \mathrm{E}[S_{\mathrm{S}}] = \mathrm{var}(S_{\mathrm{S}}) = \sum_{i}^{n_{pix}} \lambda_{\mathrm{S},i},$$
$$\mathrm{E}[N_{\mathrm{D}}] = \mathrm{var}(N_{\mathrm{D}}) = \sum_{i}^{n_{pix}} \lambda_{\mathrm{D},i}. \tag{4}$$

When taking a summation over the single pixels, it is assumed that the pixels are independent (hypothesis 2). In the classical formulation of the CCD equation as well as in the formulation of Merline, the truncation noise is modeled by an independent uniform random variable with support $[-\frac{g}{2}, \frac{g}{2}]$, where g is the gain. Newberry (1991) (hypothesis 3), where U_i are independent and identically distributed (iid) uniform random variables with support $[-\frac{g}{2}, \frac{g}{2}]$. The readout error is chosen modeled by a centered Gaussian distribution with variance $\sigma^2_{\mathrm{R},i}$ in the classical formulation and in the formulation by Merline Merline and Howell (1995) (hypothesis 4). Hence, the truncation and the readout noise variance is:

$$\mathrm{var}(N_{\mathrm{U},i}) = \frac{g^2}{24} \qquad \mathrm{var}(N_{\mathrm{R},i}) = \sigma^2_{\mathrm{R},i} \tag{5}$$

If it is assumed that all noise sources are independent (hypothesis 5), then the noise $\mathrm{var}(N_{\mathrm{classic}})$ can be deduced from Eq. (3) :

$$\begin{aligned} \mathrm{var}(N_{\mathrm{classic}}) &= \sum_{i}^{n_{pix}} \mathrm{var}(S_{\mathrm{obj},i}) + \sum_{i}^{n_{pix}} \mathrm{var}(S_{\mathrm{S},i}) + \sum_{i}^{n_{pix}} \mathrm{var}(N_{\mathrm{D},i}) \\ &\quad + \sum_{i}^{n_{pix}} \mathrm{var}(N_{\mathrm{R},i}) + \sum_{i}^{n_{pix}} \mathrm{var}(N_{\mathrm{U},i}) \qquad (6) \\ \mathrm{var}(N_{\mathrm{classic}}) &= \sum_{i}^{n_{pix}} \lambda_{\mathrm{obj},i} + \sum_{i}^{n_{\mathrm{pix}}} \lambda_{\mathrm{S},i} + \sum_{i}^{n_{\mathrm{pix}}} \lambda_{D,i} + \sum_{i}^{n_{\mathrm{pix}}} \sigma^2_{R,i} + \sum_{i}^{n_{\mathrm{pix}}} \frac{g^2}{24} \qquad (7) \end{aligned}$$

The classical formulation of the CCD equation hence results in the following expression, assuming a uniform background underneath the object image, allowing to multiply the background sources by n_{pix} rather than performing a direct summation (hypothesis 6):

$$\begin{aligned} \mathrm{SNR}_{\mathrm{classical}} &= \frac{\mathrm{E}[S_{\mathrm{obj}}]}{\sqrt{\mathrm{var}(S_{\mathrm{obj}}) + n_{\mathrm{pix}} \cdot (\mathrm{var}(S_{\mathrm{S},i}) + \mathrm{var}(N_{\mathrm{D},i}) + \mathrm{var}(N_{\mathrm{R},i}) + \mathrm{var}(N_{\mathrm{U,i}}))}} \\ &= \frac{\sum_i^{n_{\mathrm{pix}}} \lambda_{\mathrm{obj},i}}{\sqrt{\sum_i^{n_{\mathrm{pix}}} \lambda_{\mathrm{obj},i} + n_{\mathrm{pix}} \cdot (\lambda_{\mathrm{S},i} + \lambda_{\mathrm{D},i} + \sigma_{R,i}^2 + \frac{g^2}{24})}} \end{aligned} \tag{8}$$

In the classical CCD equation, the background subtraction is not included in the noise. It is equivalent to assuming that the background is perfectly determined (hypothesis 7). In the classical CCD equation and the derivation of Merline, it is furthermore assumed that the number n_{pix} of object pixels is exactly known (hypothesis 8).

The CCD equation derived by Merline and Howell (1995) differs from the classical derivation as it takes into account the background estimation process that generates additional uncertainty. In practice, the background subtraction leads to an additional term coming from the background estimation noise. In the case of a constant background, the background is estimated over the region in which the object image is located, background signal N_{B} is:

$$N_{\mathrm{B}} = \frac{1}{n_{\mathrm{B}}} \sum_i^{n_{\mathrm{B}}} (S_{\mathrm{S},i} + D_i + R_i + U_i) \tag{9}$$

and n_B is the number of background pixels used to estimate the background. A common way of estimating the background is the background pixel identification method explained in Schildknecht et al. (1995). The CCD image is divided into groups of m cells. In every group, the cells are ranked according to their intensity. Then the p lowest intensity cells and the p highest intensity cell are dropped. The background is defined as the mean intensity of the remaining pixels. The size of the sub-frame should ideally be much larger than the signal. This leads to the following modification of the noise variance compared to the classical formulation, assuming the signal is independent of the background (hypothesis

9):

$$\mathrm{var}(N_{\mathrm{Merline}}) = \mathrm{var}(N_{\mathrm{classical}}) + \frac{n_{\mathrm{pix}}}{n_{\mathrm{B}}}\mathrm{var}(N_{\mathrm{B}}) \tag{10}$$

Based on the Central Limit Theorem, the distribution of the background estimation noise can be assumed to be Gaussian, denoting $\sigma_B^2 = \mathrm{var}(N_{\mathrm{B}})$ Leading to the modified CCD equation of Merline:

$$\begin{aligned} & \mathrm{SNR}_{\mathrm{Merline}} \\ = & \frac{\mathrm{E}[S_{\mathrm{obj}}]}{\sqrt{\mathrm{var}(S_{\mathrm{obj}}) + +n_{\mathrm{pix}}\left(1+\frac{1}{n_b}\right)\cdot(\mathrm{var}(S_{\mathrm{S},i}) + \mathrm{var}(N_{\mathrm{D},i}) + \mathrm{var}(N_{\mathrm{R},i}) + \mathrm{var}(N_{\mathrm{U,i}}))}} \\ = & \frac{\sum_i^{n_{\mathrm{pix}}} \lambda_{\mathrm{obj},i}}{\sqrt{\sum_i^{n_{\mathrm{pix}}} \lambda_{\mathrm{obj},i} + n_{\mathrm{pix}}\left(1+\frac{1}{n_b}\right)(\lambda_{\mathrm{S},i} + \lambda_{\mathrm{D},i} + \sigma_{R,i}^2 + \frac{g^2}{24})}} \end{aligned} \tag{11}$$

2.1.1. Discussion of the Hypotheses of the Classical and Merline CCD Equation

In this section, we discuss the hypotheses used in the previous derivations of the CCD equations.

Hypothesis 1 - the number of electrons emitted after the absorption of photons is a Poisson random variable:. This assumption is plausible and is a classical model for electron emission. although non-Poisson distributed higher order effects exist Walter (2015).

Hypothesis 2 - the pixels are uncorrelated: As long as the Poisson parameter λ_{obj} can be modeled as a deterministic value, the pixels can be safely viewed as independent. The light reflected upon the object can be modeled using geometric optic macroscopic laws under the assumption that the object and the illumination and observation geometry is known. However, atmospheric disturbance modeling could impose using to non-deterministic Poisson parameter, depending on the level of accuracy modeling. Furthermore, in a few particular cases with very high pixel intensity, bleeding effects can occur, and in this case, neighbor pixels may be correlated Barrett et al. (2007) for example in the brighter-wider effect Lage et al. (2017); Beamer et al. (2015).

Hypothesis 3 - the truncation noise is an independent additive uniform noise: During the truncation process the signal is converted from electrons into ADU. This conversion leads to losses in resolution: the CCD can only count a limited number of electrons at the time. This assumption is conceptually wrong and leads to inaccurate estimations of the truncation noise for faint signals (cf section 2.2 for more details), besides it implies that the signal remains a Poisson distribution after the round off error.

Hypothesis 4 - the readout noise is an independent additive Gaussian noise: The readout error is a sum of independent random variables each accounting for a flaw in the electronics. The almost Gaussian distribution usually obtained Massey and George (1992) can be justified by Lindeberg-Feller theorem. Under mild assumptions on the U_i such as finite second moment, we have Durrett (2010) $\sum_i^\infty U_i$ is normally distributed.

Hypothesis 5 - the background, signal and dark noise are independent: Independence is an accurate model since the electron emissions are emitted by different and independent sources, however an intense electric current increases temperature by Joule dissipation leading to an increase in the dark noise, which is usually not the case in a cooled sensor.

Hypothesis 6 - the background is constant over the signal: Some studies such as Schildknecht et al. (1995) propose more refined models of backgrounds. For instance, due to optical effects the background may be intense at the center of the image and celestial sources such as stars may vary from pixel to pixel, however for signal of reasonable size, the variation of the background are usually negligible or can normally be counterbalanced by estimating different background values for different parts of the image.

Hypothesis 7 - the background is perfectly determined: This assumption that is assumed in the classical CCD equation and has been improved upon by Merline and Howell (1995), is wrong in general since only a limited number of pixels available to evaluate the estimated quantity of the background level.

Hypothesis 8 - the number of signal pixels is perfectly known: The diffraction pattern of the signal from the object of interest spreads the whole image frame,

same as the background pixels. In general, the object image, the first maximum of the diffraction pattern, the so-called Airy disk, is denoted as signal pixels, discriminated against the background pixels, outside the Airy disk. Sometimes, they are also called the signal and background mask. As with the background estimation, the number of pixels that belong to the object is determined as the number of pixels above the background level. Especially for very faint signals, this assumption is problematic. In this case, it may be impossible to determine for some pixels whether they should be included in the background mask or considered as part of the signal. This problem will be assessed in the derivation of the improved CCD equation in the following section.

Hypothesis 9 - the background is independent of the object signal: This appears to be legitimate as the signals stem from different sources. However, the true refraction pattern from the object signal is spreading across the whole frame, while the first order maximum, Airy disk, is usually associated with object signal, the secondary maxima are often included in the background determination (see hypothesis 8). A correlation between the background and the signal always exists. The correlation is especially significant when a sub-frame technique is utilized, using only a small number of background pixels around the trace of the object.

2.2. Derivation under more General Conditions: Improved CCD Equation

The derivation of the improved CCD equation is based upon the derivation of Merline and Howell (1995). The hypotheses 3 and 8 are relaxed: The modeling of the truncation error is improved upon Merline's formulation, and the uncertainty in the number of object pixels is taken into account. Improvements are most significant for faint object images with a low SNR, such as the one shown in Fig. 3. A summary of the hypotheses used in each derivation is given in Table 1.

First, we work on the truncation error term. To avoid the assumption of a uniform distribution, the signal after truncation has to be defined. Taking the Poisson processes, stemming from the actual photon impacts, we use the

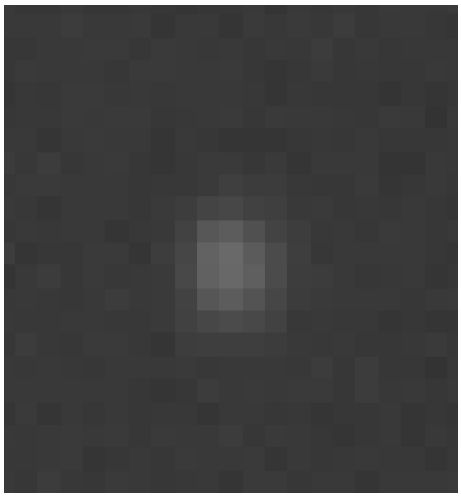

Figure 3: Example of a faint signal with low signal-to-noise ratio (source Purdue Optical Ground Station).

following notation for the independent Poisson signals S_{pois}:

$$S_{\text{pois},i} = S_{\text{obj},i} + S_{\text{S},i} + N_{\text{D},i} \tag{12}$$

We also define for later use, the Poisson signals excluded the object signal:

$$S_{\text{SD},i} = S_{\text{S},i} + N_{\text{D},i} \tag{13}$$

The corresponding truncated signal is denoted by $S_{\text{pois,trunc},i}$. In contrast to the approximate representation in the previous section, $S_{\text{pois,trunc},i}$ is no longer a Poisson distributed random variable. In the following, we derive the exact distribution of the signal after the truncation. For simplicity, we assume here that the gain g is even. We get for the probability of the truncated signal $S_{\text{pois,trunc},i}$ based on the original signal in the interval subject to truncation, $S_{\text{pois},i}$, for any signal strength q:

$$P(S_{\text{pois,trunc},i} = q) = P\left(S_{\text{pois},i} \in \left[g\left(q - \frac{1}{2}\right); g\left(q + \frac{1}{2}\right)\right]\right) \quad \text{for any } q > 0. \tag{14}$$

Hypotheses	classical CCD equation	Merline's CCD equation	Improved CCD equation
Hypothesis 1	X	X	X
Hypothesis 2	X	X	X
Hypothesis 3	X	X	
Hypothesis 4	X	X	X
Hypothesis 5	X	X	X
Hypothesis 6	X	X	X
Hypothesis 7	X		
Hypothesis 8	X	X	
Hypothesis 9	X	X	X

Table 1: Summary of the hypotheses used in the derivation of the different CCD equations presented in this work. The 'X' means the hypothesis is used to derive the SNR. Hence the fewer 'X's, the better. The hypotheses are presented and discussed in Section 2.1.1

This is equivalent to:

$$P(S_{\text{pois,trunc},i} = q) = \sum_{k=gq}^{g(q+1)-1} \frac{\exp(-\lambda_{\text{pois},i})\lambda_{tot,i}^{k-\frac{1}{2}g}}{(k-\frac{g}{2})!} = \frac{\Gamma(g(q+\frac{1}{2}),\lambda_{\text{pois},i})}{\Gamma(g(q+\frac{1}{2}))} - \frac{\Gamma(g(q-\frac{1}{2}),\lambda_{\text{pois},i})}{\Gamma(g(q-\frac{1}{2}))}, \tag{15}$$

for any $k > 0$. $\Gamma(q) = (q-1)!$ is the Gamma function and $\Gamma(q,x) = \int_x^\infty e^{-t}t^{q-1}dt$ is the incomplete Gamma function. The noise variance of the Poisson sources, $\text{var}(S_{\text{pois,trunc},i})$ can be derived using the previous analytical expression of $P(S_{\text{pois},i} = q)$ in Eq.14:

$$\text{var}(S_{\text{pois,trunc},i}) = \sum_{q>0} q^2 P(\text{var}(S_{\text{pois},i}) = q) - \left(\sum_{q>0} qP(\text{var}(S_{\text{pois},i}) = q)\right)^2 \tag{16}$$

In the next step, the background subtraction is more closely investigated.

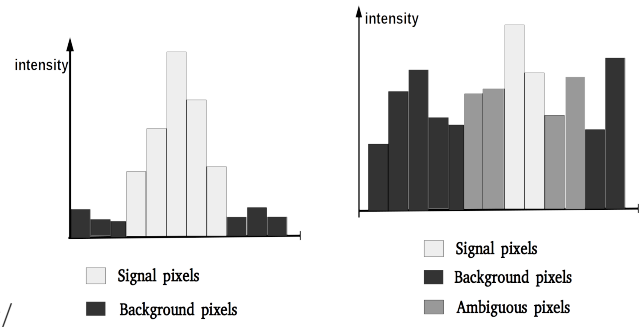

fig/

(a) Schematic of non-ambiguous signal: the signal pixels clearly stand above the background level

(b) Example of ambiguous signal: it is unclear for some pixels whether they belong to the signal or not

Figure 4: Signals with and without ambiguous pixels

As previously discussed, there is indeed a correlation between the background and the object image. This correlation is exacerbated for very faint object traces relative to the (true) background, in which cases also the Airy disk's main maximum may merge with the surrounding background. Fig. 3 gives an example of a very faint signal where the pixels at the edge of the signal are extremely ambiguous. Ambiguous pixels are those pixels that could be part of the object image or part of the background. The following CCD equation derivation accounts for the ambiguous pixels that can be part of the signal, in terms of the first Airy disk or signal mask, and of the background, respectively background mask. We denote $I_{\rm amb}$ the set of ambiguous pixels. The ambiguous pixels are included in the background mask and are considered as being part of the signal. In other words we have $I_{\rm amb} \subset I_{\rm obj}andI_{\rm amb} \subset I_{\rm B}$, where $I_{\rm obj}$ is the set of signal pixels from the object image and I_B is the set of background pixels used in the background determination. Note that in our model the membership of each pixel $I_{\rm amb}$, $I_{\rm obj}$ or $I_{\rm B}$ is deterministic and not subject to uncertainty. The overall actual background B (analogous to Eq.(9)) can readily be defined

as:

$$N_{\mathrm{B}} = \frac{1}{n_B}\sum_{i}^{n_{\mathrm{B}}} S_{\mathrm{pois},i} + N_{\mathrm{U},i} + N_{\mathrm{R},i} = \frac{1}{n_B}\sum_{i}^{n_{\mathrm{B}}} S_{\mathrm{pois,trunc},i} + N_{\mathrm{R},i}$$
$$= \frac{1}{n_B}\sum_{i}^{n_{\mathrm{B}}} N_{\mathrm{total},i} \tag{17}$$

B and S_{pois} are correlated since the some pixels are used to compute B and S. As a result the background subtracted image noise is:

$$N_{\mathrm{impro}} = S_{\mathrm{pois}} - n_{\mathrm{pix}}B = \sum_{i\in I_{\mathrm{obj}}} N_{\mathrm{total},i} - \frac{n_{\mathrm{pix}}}{n_B}\sum_{i\in I_B} N_{\mathrm{total},i} \tag{18}$$

$$N_{\mathrm{impro}} = \sum_{i\in I_{\mathrm{obj}}\setminus I_{\mathrm{amb}}} N_{\mathrm{total},i} + (1-\frac{n_{\mathrm{pix}}}{n_{\mathrm{B}}})\sum_{i\in I_{\mathrm{amb}}} N_{\mathrm{total},i}$$
$$-\frac{n_{\mathrm{pix}}}{n_{\mathrm{B}}}\sum_{i\in I_{\mathrm{B}}\setminus I_{\mathrm{amb}}} N_{\mathrm{total},i} \tag{19}$$

where n_{pix} are the number of object trace pixels (including the unambiguous and the ambiguous pixels) , n_{amb} are the ambiguous trace pixels that could belong either to the object trace's first maximum or the background, n_B are the number of pixels used in the background estimation. Then the noise variance can be computed as :

$$\mathrm{var}(N_{\mathrm{impro}}) = \sum_{i\in I_{\mathrm{obj}}\setminus I_{\mathrm{amb}}} \mathrm{var}(S_{\mathrm{pois,trunc},i}) + (1-\frac{n_{\mathrm{pix}}}{n_{\mathrm{B}}})^2\sum_{i\in I_{\mathrm{amb}}} \mathrm{var}(S_{\mathrm{pois,trunc},i})$$

with $n = (n_{\mathrm{pix}} - 2\frac{n_{amb}n_{\mathrm{pix}}}{n_B} + \frac{n_{\mathrm{pix}}^2}{n_B})$. Finally this leads to the improved CCD equation:

$$\mathrm{SNR}_{\mathrm{impro}} = \frac{\mathrm{E}[S_{\mathrm{obj}}]}{\sqrt{\mathrm{var}(N_{\mathrm{impro}})}}$$
$$= \frac{\mathrm{E}[S_{\mathrm{obj}}]}{\sqrt{\sum_{i\in I_{\mathrm{obj}}\setminus I_{\mathrm{amb}}} \mathrm{var}(S_{\mathrm{pois,trunc},i}) + (1-\frac{n_{\mathrm{pix}}}{n_B})^2\sum_{i\in I_{\mathrm{amb}}} \mathrm{var}(S_{\mathrm{pois,trunc},i})}}$$
$$\overline{\qquad\qquad\qquad\qquad\qquad\qquad\qquad\qquad\qquad\qquad\qquad\qquad\qquad\qquad\qquad\qquad}$$
$$\overline{+\left(\frac{n_{\mathrm{pix}}}{n_B}\right)^2\sum_{i\in I_B\setminus I_{\mathrm{amb}}} \mathrm{var}(S_{\mathrm{pois,trunc},i}) + n\cdot\mathrm{var}(N_{\mathrm{R},i})} \tag{20}$$

denoting as before with $\lambda_{\mathrm{obj},i}$ the corresponding Poisson parameter of the object signal and with $\sigma^2_{\mathrm{R,i}}$ the Gaussian variance of the readout noise in the ith pixel,

respectively.

$$\mathrm{SNR}_{\mathrm{impro}} = \frac{\sum_i^{n_{\mathrm{pix}}} \lambda_{\mathrm{obj},i}}{\sqrt{\sum_{i\in I_{\mathrm{obj}}\setminus I_{\mathrm{amb}}} \mathrm{var}(S_{\mathrm{pois,trunc},i}) + (1-\frac{n_{\mathrm{pix}}}{n_B})^2 \sum_{i\in I_{\mathrm{amb}}} \mathrm{var}(S_{\mathrm{pois,trunc},i})}} \\ \overline{+\left(\frac{n_{\mathrm{pix}}}{n_B}\right)^2 \sum_{i\in I_B\setminus I_{\mathrm{amb}}} \mathrm{var}(S_{\mathrm{pois,trunc},i}) + n\cdot\sigma^2_{\mathrm{R},i}} \quad (21)$$

Assuming that all the Poisson distribution parameters S_{pois} are constant, the expression can be simplified to the following:

$$\mathrm{SNR}_{\mathrm{impro,const}} = \frac{\sum_i^{n_{\mathrm{pix}}} \lambda_{\mathrm{obj},i}}{\sqrt{(n_{\mathrm{pix}} - \frac{2n_{\mathrm{amb}}n_{\mathrm{pix}}}{n_{\mathrm{B}}} + \frac{n_{\mathrm{amb}}n^2_{\mathrm{pix}}}{n^2_{\mathrm{B}}})\mathrm{var}(S_{\mathrm{pois,trunc}})}} \\ \overline{+(\frac{n_{\mathrm{pix}}}{n_{\mathrm{B}}})^2(n_{\mathrm{B}}-n_{\mathrm{amb}})\mathrm{var}(S_{\mathrm{SD,trunc}}) + n\cdot\sigma^2_{\mathrm{R}}}$$

Where $\mathrm{var}(S_{\mathrm{SD}})$ is the variance of the Poisson signals without light from the object trace S_{pois} (see definition in Eq.(13)). The truncated version of S_{SD} is denoted $S_{\mathrm{SD,trunc}}$. Its variance is computed using Eq. (16).

Further simplifications can be proposed if the number of signal pixels is much smaller than the number of pixels used for the background determination. In that case, the ratio $\frac{n_{amb}}{n_B}$ is small and the background is well determined. In this case we can take $\frac{n_{amb}}{n_B} \to 0$ in Eq. (22):

$$\mathrm{SNR}_{\mathrm{impro,const}} \approx \frac{\sum_i^{n_{\mathrm{pix}}} \lambda_{\mathrm{obj},i}}{\sqrt{\frac{n_{\mathrm{pix}}}{nB}\mathrm{var}(S_{\mathrm{SD,trunc}}) + n_{\mathrm{pix}}\mathrm{var}(S_{\mathrm{pois,trunc}}) + (1+\frac{n_{\mathrm{pix}}}{n_B})\sigma^2_{\mathrm{R}}}}. \quad (22)$$

The equation is similar to Merline and Howell (1995) except for the modeling of the truncation noise. If the number of background pixel is small (a sub-frame technique has been used to reach a higher sampling rate) or the signal is faint, then Eq. (22) is more accurate.

If the truncation error is modeled in the traditional way, assuming a uniform distribution, the simplified improved CCD equation Eq. (22) is identical to Merline's CCD equation Eq. (11).

3. Probability of Detection

The probability of detection is a probability measure of how likely one is to detect an object whose image is indeed in the field of view, that is, present in the CCD frame. It is immediately clear that the probability of detection is directly related to the signal of the object image in comparison to the background of the frame. Several approaches for space object detection have been proposed using segmentation methods Virtanen et al. (2016) where pixels above a given intensity are considered, Gaussian convolution Schildknecht et al. (2015), suited space transforms (Radon or Hough) Ciurte and Danescu (2014); Zimmer et al. (2013). Most detection algorithms rely on the entire object signal to detect the object (or even several images Yanagisawa et al. (2012)), and when computed, the probability of detection relies on a Gaussian noise assumption. Using several pixels to declare detection may be used in large faint streaks and permits to use a lower detection threshold. However, for faint and small signals, the probability of detection may rely on only one pixel. Faint and small signals are of particular interest because the detection probability is significantly lower than one. The derivation proposed in the following paragraph assumes only one pixel is used to declare detection, but it can be extended to detection strategies using multiple pixels.

In the following, we define the probability of detection via a single pixel only, instead of the whole object image. Naturally, the brightest pixel is selected. The underlying idea is that the brightest pixel is more crucial for the detection than any part of the object image. It is, of course, noted that the theoretically brightest pixel in the center of the Airy disk might not be the brightest pixel in the realization of the stochastic process on the pixel grid. When spatial filters are applied, the brightest pixel after filter application is to be used.

Depending on the specific image processing method used, a particular threshold t between the background and the object image signal is set, above which detection

is possible. Potent image processing algorithms can reach a threshold of 2.5 Houtz and Frueh (2018). Hence, we define the probability of detection P_d for a given threshold:

$$\begin{aligned} P_\mathrm{d} = \quad & P(S_{\mathrm{obj,trunc},i_\mathrm{bpix}} > t) \\ & + P(S_{\mathrm{obj,trunc},i_\mathrm{bpix}} < t \text{ at least one other j has } S_{\mathrm{obj},j} > t), \end{aligned} \tag{23}$$

where $S_{\mathrm{obj,trunc},i_\mathrm{bpix}}$ is the signal of the expected brightest pixel of the object image. It is the measured signal and therefore includes the signal itself and the background noise, both truncated, plus the readout noise. In practice, if the brightest pixel is brighter than the other signal pixels, the second term is small. In the following derivation, it is neglected. For the rest of the derivation, it is implicit that only the brightest pixel is considered. If we use the signal definition from Eq.(17), we can express the probability of detection as:

$$P_\mathrm{d} = 1 - P(S_{\mathrm{pois,trunc},i_\mathrm{bpix}} - N_{\mathrm{B},i_\mathrm{bpix}} + N_{\mathrm{R},i_\mathrm{bpix}} < t). \tag{24}$$

Computing $P(S_{\mathrm{pois,trunc},i_\mathrm{bpix}} - N_{\mathrm{B},i_\mathrm{bpix}} + N_{\mathrm{R},i_\mathrm{bpix}} < t)$. can be complex and numerically expensive. Reasonable simplifications are proposed in order to explicate this expression. If the number of background pixels is large enough the central limit theorem allows us to approximate N_B with a Gaussian random variable with mean $\mu_B = E[S_{\mathrm{SD,trunc}}]$ and variance $var(S_{\mathrm{SD,trunc}}) = \sigma_B^2$. Moreover, $-N_\mathrm{B} + N_\mathrm{R}$ is the sum of two independent Gaussian random variables which is also a Gaussian random variable with mean $-\mu_\mathrm{B}$ and variance $\sigma_R^2 + \sigma_B^2$. Under those assumptions the probability of detection becomes, separating the Gaussian distributed parts with respect to the brightest pixel i_bpix:

$$P_\mathrm{d} = 1 - \int P(S_{\mathrm{pois,trunc},i} - \epsilon < t | - B_i + N_{\mathrm{R},i} = \epsilon) P(N_{\mathrm{B},i} - N_{\mathrm{R},i} = -\epsilon) d\epsilon \quad \text{for } \; i = i_\mathrm{bpix}$$

Based on the definition of $S_{\mathrm{pois,trunc},i}$ Eq. 14 and from the fact that$S_{\mathrm{pois},i}$ is

assumed to be Poisson distributed, we obtain:

$$\begin{aligned} &P(S_{\text{pois,trunc},i} - \epsilon < t| - N_{\text{B},i} + N_{\text{R},i} = \epsilon) \\ &\quad = P(S_{\text{pois,trunc},i} - \leq \lfloor t + \epsilon \rfloor) \\ &\quad = P(S_{\text{pois},i} - \leq g\lfloor t + \epsilon \rfloor - \frac{g}{2}) \\ &\quad = \frac{\Gamma(g\lfloor t + \epsilon \rfloor - \frac{g}{2}, \lambda_{\text{obj},i} + \lambda_{\text{S},i} + \lambda_{\text{D},i})}{(g\lfloor t + \epsilon \rfloor - \frac{g}{2})!}. \end{aligned} \tag{25}$$

$\lfloor x \rfloor$ denotes the closest integer smaller or equal to x. Without any loss of generality, the gain g is assumed to be even. Using Eq. (25) the probability of detection can be written as:

$$\begin{aligned} P_{\text{d}} =& 1 - \int_{-\infty}^{\infty} \frac{\Gamma(g\lfloor t + \epsilon \rfloor - \frac{g}{2}, \lambda_{\text{obj},i} + \lambda_{\text{S},i} + \lambda_{\text{D},i})}{(g\lfloor t + \epsilon \rfloor - \frac{g}{2})!} \\ & \cdot \frac{1}{\sqrt{2\pi(\sigma^2_{\text{B},i} + \sigma^2_{\text{R},i})}} \exp\left(-\frac{(\epsilon - \mu_{\text{B},i})^2}{2(\sigma^2_{\text{B},i} + \sigma^2_{\text{R},i})}\right) d\epsilon. \end{aligned}$$

for $i = i_{\text{bpix}}$

Eq. (26) can be simplified for any integer n as long as we have $\epsilon \in [n-t; n+1-t)$ then $\lfloor t + \epsilon \rfloor = n$:

$$\begin{aligned} P_{\text{d}} =& 1 - \frac{1}{2} \sum_{n=-\infty}^{\infty} \frac{\Gamma(n - \frac{g}{2}, \lambda_{\text{obj},i} + \lambda_{\text{S,i}} + \lambda_{\text{D,i}})}{n!} \\ & \cdot \frac{1}{\sqrt{2\pi(\sigma^2_{\text{B},i} + \sigma^2_{\text{R},i})}} \int_{\epsilon \in [n-t; n+1-t)} \exp\left(-\frac{(\epsilon - \mu_{\text{B},i})^2}{2(\sigma^2_{\text{B},i} + \sigma^2_{\text{R},i})}\right) d\epsilon \end{aligned} \tag{26}$$

$$\begin{aligned} P_{\text{d}} =& 1 - \frac{1}{2} \sum_{n=-\infty}^{\infty} \frac{\Gamma(n - \frac{g}{2}, \lambda_{\text{obj},i} + \lambda_{\text{S,i}} + \lambda_{\text{D,i}})}{n!} \\ & \cdot \left(erf\left(\frac{n + 1 - t - \mu_{\text{B},i}}{\sqrt{2g(\sigma^2_{\text{B},i} + \sigma^2_{\text{R},i})}}\right) - erf\left(\frac{n - t - \mu_{\text{B},i}}{\sqrt{2g(\sigma^2_{\text{B},i} + \sigma^2_{\text{R},i})}}\right)\right), \end{aligned}$$

for $i = i_{\text{bpix}}$

where erf is the error function. In actual computation, the n summation is approximated by limiting it to a suitable value range.

4. Results

4.1. Performance of the Improved CCD Equation

The performance of the different expressions of the CCD equations, Eq. (8), Eq. (11) and Eq. (22), is evaluated. To assess the performance of different CCD equations, we use Monte Carlo simulations as reference: a large number of CCD frames are simulated, and the average signal and noise are extracted to compute the SNR. A two-step validation is performed: in the first step, the effect of the mismodelling of the truncation error is investigated. In a second step, the different approximations of the true signal-to-noise ratio, represented in Eq. (8), Eq. (11) and Eq. (22) are compared against the Monte Carlo results, and their performance is quantified. In the Monte Carlo simulation of the CCD frames, a Gaussian noiseless signal is generated as the object image and constant background noise S_{S} is added to it. Then, the photo-electron release by the external sources and internal dark noise is simulated. In the simulation of the readout process, the readout noise and the truncation process are also included.

4.2. Comparison of the Noise Models for the Truncation Error

In this section the truncation error modelling as uniform variable, Newberry (1991); Merline and Howell (1995) is compared to the improved modelling, as shown in section 2. The noise for a truncated signal has been computed and plotted in three different ways in Fig. 5 to optimally illustrate the difference between the two noise models. In this set of tests, the variances have been computed only considering the truncation noise and stochastic electron emission noise. The signal variance denoted by $\mathrm{var}_{\mathrm{MC}}$, is obtained running 100,000,000 independent identically Poisson distributed samples of parameter λ, rounding off the signal and computing the variance of the signal. The second one is computed using the expression derived in the previous section (see Eq. (15)):

$$\begin{aligned} \mathrm{var}_{\mathrm{impro}} &= \sum_{m=1}^{\infty} m^2 P(S_{\mathrm{trunc}} = m) - \left(\sum_{m=1}^{\infty} m P(S_{\mathrm{trunc}} = m) \right)^2 \\ \text{with } P(S_{\mathrm{trunc}} = m) &= \sum_{k=gm}^{g(m+1)-1} \frac{exp(-\lambda)\lambda^{k-\frac{1}{2}g}}{(k-\frac{g}{2})!}. \end{aligned} \tag{27}$$

Finally the third expression, noted $\mathrm{var}_{\mathrm{classical}}$, is computed as in the literature Merline and Howell (1995):

$$\mathrm{var}_{\mathrm{classical}} = \lambda + \frac{g^2 - 1}{12}, \tag{28}$$

where $\frac{g^2-1}{12}$ is the variance of a uniformly distributed random variable. Fig. 5

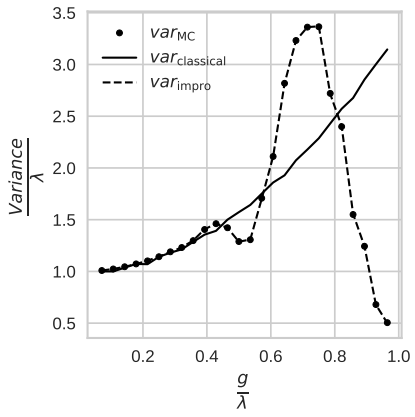

Figure 5: Comparison of the truncation noise for $\mathrm{var}_{\mathrm{MC}}$, $\mathrm{var}_{\mathrm{impro}}$ and $\mathrm{var}_{\mathrm{classical}}$. The variances are normalized by the variance of the Poisson signal λ.

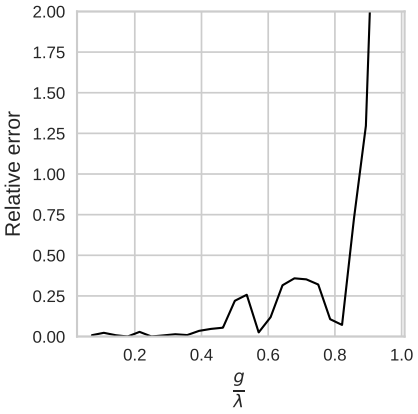

Figure 6: Relative error between the exact variance of the truncated signal and the approximated variance V_{approx}.

shows that the improved model of truncation noise performs better than the approximation used in literature, especially for faint signals with high gain. Fig. 6 displays the relative error between $\mathrm{var}_{\mathrm{MC}}$ and $\mathrm{var}_{\mathrm{impro}}$. It shows that when the signal is only three times bigger than the gain, the approximation used in the literature becomes inaccurate. Hence, the approximation made by Merline and Howell (1995) and Newberry (1991) is acceptable for very bright star observations, where $\frac{g}{\lambda}$ is small. For faint signals, the ratio $\frac{g}{\lambda}$ may be much higher, and the improved expression of the noise for the truncation error should be used.

4.2.1. Comparison of the CCD Equations for Signals without Ambiguous Pixels

Now, the full expressions of the CCD equations, approximating the SNR of the image frame, Eq. (8), Eq. (11) and Eq. (22), are compared to Monte Carlo simulations. It is assumed that all object image pixels (Airy disc) are perfectly identified and discriminated against the background. Fig. 1 shows an illustrative example of a signal in which the object pixels can be easily identified, as the signal-to-noise ratio (SNR) in all object pixels is high. Fig. 7 shows the performance of the three approximations of the true SNR: the classical CCD equation, Merline's CCD equation as presented in Merline and Howell (1995) and the improved CCD equation (see Eq. (22)) as a function of the normalized background level. The background is normalized by the expected intensity of the expected brightest pixel. All three are compared to a Monte Carlo estimation of the SNR obtained with 50 000 samples. The classical formulation is different. The Monte Carlo simulation results are in good agreement with the improved and Merline CCD equation formulations while the classical formulation is biased. The difference seems to be constant and is about 1 in the SNR. The constant offset is due to the background estimation noise that is neglected in the classical formulation.

4.2.2. Comparison of the Signal-to-noise ratio for Signals with Ambiguous Pixels

The situation is different when the presence of ambiguous pixels is taken into account. As the signal can be extremely faint, it may become extremely difficult to tell whether a pixel belongs to the background or the signal (see Fig. 3 and 4b). Furthermore, in some cases, where very few pixels are available to compute the background, one is likely to include those ambiguous pixels in their estimation of the background level. In practice, the ambiguous pixels are pixels for which the intensity from the observed object is of the same order of magnitude as the background noise.

Fig. 8 shows again, the three formulations of the SNR as given in the three formulations of the CCD equation and the Monte Carlo simulation obtained with

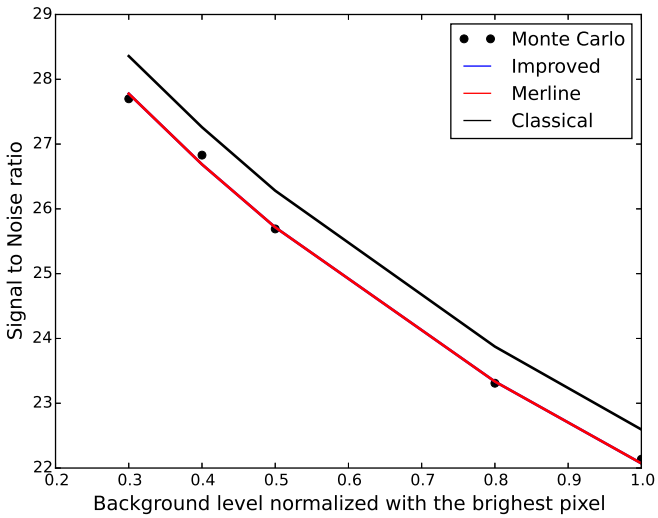

Figure 7: Evolution to signal-to-noise ratio as a function if read out noise for $g = 0.06\lambda_{\text{obj}}$, no ambiguous pixels are present.

50 000 samples. Note that the ambiguous pixels are modeled as a deterministic quantity. Now, a clear distinction between all three formulations is visible. The improved formulation now lies in-between the SNR values estimated by the classical and the estimation from Merline and Howell (1995). The differences appear to be constant. The constant offsets are according to the constant offset introduced by neglecting the background estimation noise in the classical formulation and the constant amount of ambiguous pixels that are simulated. The Monte Carlo simulations align almost perfectly with the improved formulation. One particular result is that the introduction of ambiguous pixels does not necessarily lower the signal-to-noise ratio since the membership of the ambiguous pixels is deterministic. In practice, the difficulty behind differentiating the signal pixels from the background pixels makes the classical definition of the signal-to-noise ratio extremely ambiguous and subject to the observer subjectivity. It is hence more adequate to take the ambiguous pixels into account.

In this test, the number of ambiguous pixels considered is kept constant to facilitate the comparison between the three approaches. For lower SNR values, the number of ambiguous pixels is expected to increase, and therefore the difference between our estimation of the SNR and Merline's estimation is expected to grow.

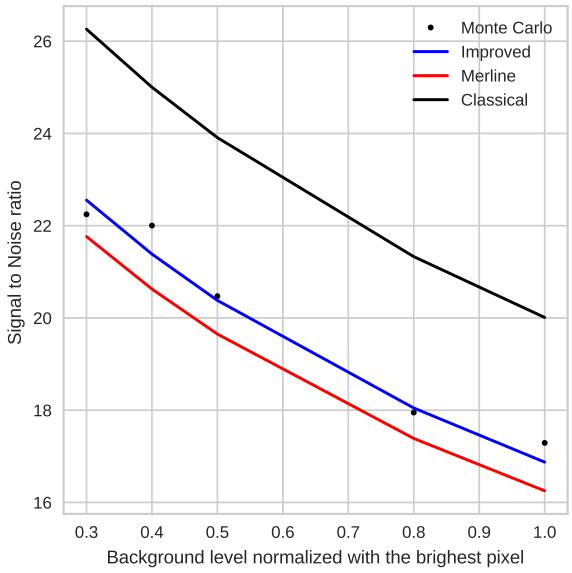

Figure 8: Evolution to signal-to-noise ratio as a function of normalized background level ($g = 0.06\lambda_{\text{obj}}$) with ambiguous pixels present.

Note: When computing the probability of detection (see nex section), the difference between the formulation of Merline (Merline and Howell, 1995) and the improved CCD equation can be limited even in cases of ambiguous pixels, since only the brightest pixel is taken into account.However, in practice, (in contrast to the use in probability of detection) the SNR of the whole object image is often of interest.

4.3. Validation of the Probability of Detection

To validate the expression for the probability of detection, derived in Eq. (27), the results are compared to 500 000 Monte Carlo simulations. As the choice of t is not unique but ultimately user-defined, the results are shown in Fig. 9 for different values of t. t is chosen as $k \times N$, where N is the noise. The value of the threshold should be chosen such as it minimizes the risk of false detection and maximize the number of space objects detected. Fig. 9 shows the excellent agreement of the expression for the probability of detection with all Monte Carlo simulations, despite approximations that have been made to permit fast computationally efficient computations. The analytical expressions can be used in multi-target tracking scenarios. Note that the computation of the probability of detection does not require to model the ambiguous pixels as for the CCD equations. Moreover, it is possible to compute the probability of detection accurately, without using the CCD equation representation. Sometimes the SNR computation is not of interest once the probability of detection is accurately determined.

Note, that also the Monte Carlo validation also considers only the expected brightest pixel when estimating the probability of detection. This hypothesis is valid as t is chosen to minimize false positives.

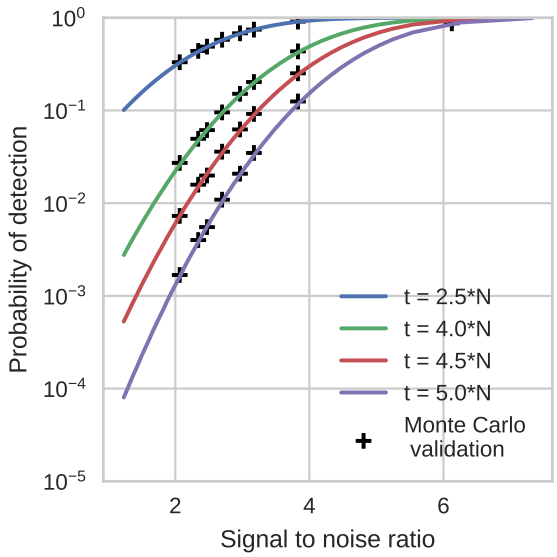

Figure 9: Detection probability as a function of the signal-to-noise ratio (SNR).

5. Conclusions

In this work, the signal-to-noise ratio and the probability of detection of non-resolved object images on Charged Coupled Device (CCD) sensors are investigated. Non-resolved object images cover only a few pixels and do not feature any details of the object itself. The application cases in this paper are optical ground-based observations of human-made space objects. The results are, however, not specific to those observations.

Sensing is affected by external light sources entering the detector, but also internal detector noise. The detection process itself is stochastic. As a result, the signal-to-noise ratio can only be correctly computed using computationally intensive Monte Carlo simulations. Approximate expressions of the signal-to-noise ratio, so-called, CCD equation exist in literature. In this work, two common CCD equations and the modeling hypothesis they are based on are discussed. In a generalized approach, an improved CCD equation is derived. It features two

modeling improvements. Firstly, it accurately models the truncation noise rather than using a uniform approximation. Secondly, the generalized formulation does not assume that the object image pixels above the background are perfectly known. Instead, the notion of ambiguous pixels is introduced. Avoiding the latter assumption proved to have a significant impact. The validation results showed that if the object image is intensity is comparable to the background, and if some pixels can be classified as *ambiguous pixels*, belonging to the background or the object image, the improved CCD equation compares significantly better to the Monte Carlo ground truth. In case no ambiguous pixels are present, the performance is the same as the CCD equation first proposed by Merline and Howell (1995).

Based on the improved representation of the object signal and the background, an expression for the probability of detection has been derived. A computationally fast analytic approximation has been provided. The approximation is in excellent agreement with the Monte Carlo simulated ground truth. The expression for the probability of detection avoids the explicit computation of the CCD equation. Both, the analytical expressions of the detection probability, and the improved CCD equation cut down computational cost avoiding expensive Monte Carlo simulations.
In this work, the expressions derived were compared to Monte Carlo simulations, future work could focus on further comparing our formulation to real observations, in particular using well-characterized stars.

6. Acknowledgements

We would like to acknowledge and thank for the support of this work via the AFSOR grant FA9550-14-1-0348 DEF.

References

Barrett, H. H., Dainty, C., Lara, D., 2007. Maximum-likelihood methods in wavefront sensing: stochastic models and likelihood functions. JOSA A 24 (2), 391–414.

Beamer, B., Nomerotski, A., Tsybychev, D., may 2015. A study of astrometric distortions due to "tree rings" in CCD sensors using LSST photon simulator. Journal of Instrumentation 10 (05), C05027–C05027.
URL https://doi.org/10.1088%2F1748-0221%2F10%2F05%2Fc05027

Ciurte, A., Danescu, R., 2014. Automatic detection of meo satellite streaks from single long exposure astronomic images. In: 2014 International Conference on Computer Vision Theory and Applications (VISAPP). Vol. 1. IEEE, pp. 538–544.

Clark, D., Emmanuel, Delande, E., Frueh, C., 2008. Multi-Object Filtering for Space Situational Awareness. Tech. rep., Heriot-Watt University, Endinburgh.

Clark, D., Vo, B.-T., Vo, B.-N., 2007. Gaussian particle implementations of probability hypothesis density filters. In: Aerospace Conference, 2007 IEEE. IEEE, pp. 1–11.

Coder, R. D., Holzinger, M. J., 2016. Multi-objective design of optical systems for space situational awareness. Acta Astronautica 128, 669 – 684.
URL http://www.sciencedirect.com/science/article/pii/S0094576516306336

Delande, E., Frueh, C., Houssineau, J., Clark, D., 2015. Multi Object Filtering for Space Situational Awarness. AAS Space Flight Mechanics Meeting.

DeMars, K. J., Hussein, I. I., Frueh, C., Jah, M. K., Scott Erwin, R., 2015. Multiple-Object Space Surveillance Tracking Using Finite-Set Statistics. Journal of Guidance, Control, and Dynamics, 1–16.

Durrett, R., 2010. Probability: Theory and Examples. Cambridge Series in Statistical and Probabilistic Mathematics. Cambridge University Press.

Frueh, C., Fielder, H., Herzog, J., 2017. Heuristic and optimized sensor tasking observation strategies with exemplification for geosynchronous objects. Journal of Guidance, Control, and Dynamics 41 (5), 1036–1048.

Hagen, N., Dereniak, E., 2008. Gaussian profile estimation in two dimensions. Applied optics 47 (36), 6842–6851.

Houtz, N., Frueh, C., 2018. Streak detection and chatacterization in ground-based optical observations of space objects. AASAIAA Astrodynamics Specialist Conference, Snowbird, Utah, Month = August.

Howell, S., 2006. Handbook of Ccd Astronomy. Cambridge University Press.

Janesick, J. R., Elliott, T., Collins, S., Blouke, M. M., Freeman, J., 1987. Scientific charge-coupled devices.

Lage, C., Bradshaw, A., Tyson, J., mar 2017. Measurements and simulations of the brighter-fatter effect in CCD sensors. Journal of Instrumentation 12 (03), C03091–C03091.
URL https://doi.org/10.1088%2F1748-0221%2F12%2F03%2Fc03091

Mahler, R. P. S., 2007. Statistical Multisource-Multitarget Information Fusion. Artech House, Inc., Norwood, MA, USA.

Massey, P., George, H., 1992. CCD Data: The Good, The Bad, and The Ugly. In: Steve B. Howell (Ed.), Astronomical CCD observing and reduction techniques. Vol. 23. Astronomical Society of the Pacific, San Francisco, p. 240.

McCabe, J. S., DeMars, K. J., Frueh, C., 2015. Integrated Detection and Tracking for Multiple Space Objects. AAS Space Flight Mechanics Meeting.

Merline, W. J., Howell, S. B., 1995. A realistic model for point-sources imaged on array detectors: The model and initial results. Experimental Astronomy 6 (1-2), 163–210.

Mortara, L., Fowler, A., Jan. 1981. Evaluations of Charge-Coupled Device / CCD / Performance for Astronomical Use. In: Society of Photo-Optical Instrumentation Engineers (SPIE) Conference Series. Vol. 290. p. 28.

Newberry, M. V., 1991. Signal-to-noise considerations for sky-subtracted CCD data. Astronomical Society of the Pacific 103, 122–130.

Sanson, F., Frueh, C., 2015. Noise Quantification in Optical Observations of Resident Space Objects for Probability of Detection and Likelihood. In: Proc. AIAA/AAS Astrodynamic Specialist Conference. Vail, Colorado.

Sanson, F., Frueh, C., 2019. Quantifying uncertainties in signal position in non-resolved object images: Application to space object observation. Advances in Space Research 63 (8), 2436 – 2454.
URL http://www.sciencedirect.com/science/article/pii/S0273117719300067

Schildknecht, T., Hugentobler, U., Verdun, A., Beutler, G., 1995. CCD Algorithms for space debris detection. Tech. rep., University of Berne.

Schildknecht, T., Schild, K., Vannanti, A., 2015. Streak detection algorithm for space debris detection on optical images. In: Advanced Maui Optical and Space Surveillance Technologies Conference.

Smal, I., Loog, M., Niessen, W., Meijering, E., 2010. Quantitative comparison of spot detection methods in fluorescence microscopy. IEEE Transactions on Medical Imaging, 29 (2), 282–301.

Tiersch, H., 1993. S.B. Howell (ed.): Astronomical CCD observing and reduction techniques. Astronomical Society of the Pa-cific 1992, ASP Conference Series 23, 339 s., Preis: 55,-ISBN 0-937707-42-4. Astronomische Nachrichten 314 (6), 398.

Virtanen, J., Poikonen, J., Sntti, T., Komulainen, T., Torppa, J., Granvik, M., Muinonen, K., Pentikinen, H., Martikainen, J., Nrnen, J., Lehti, J., Flohrer,

T., 2016. Streak detection and analysis pipeline for space-debris optical images. Advances in Space Research 57 (8), 1607 – 1623, advances in Asteroid and Space Debris Science and Technology - Part 2.
URL http://www.sciencedirect.com/science/article/pii/S0273117715006663

Walter, C., may 2015. The brighter-fatter and other sensor effects in CCD simulations for precision astronomy. Journal of Instrumentation 10 (05), C05015–C05015.

Yanagisawa, T., Kurosaki, H., Banno, H., Kitazawa, Y., Uetsuhara, M., Hanada, T., 2012. Comparison between four detection algorithms for geo objects. In: Proceedings of the Advanced Maui Optical and Space Surveillance Technologies Conference. Vol. 1114. p. 9197.

Zimmer, P. C., Ackermann, M. R., McGraw, J. T., 2013. Gpu-accelerated faint streak detection for uncued surveillance of leo. In: Proceedings of the 2013 AMOS Technical Conference.